Femtosecond Coherent Spectroscopic Study of Zn(II)porphyrin Using Chirped Ultrashort Pulses

Min-Chul Yoon, Jae Kyu Song, Sung Cho, and Dongho Kim*

National Creative Research Initiatives Center for Ultrafast Optical Characteristics Control and Department of Chemistry, Yonsei University, Seoul 120-749, Korea

Received April 14, 2003

We have investigated femtosecond coherent vibrational motions of Zn(II)-5,15-diphenylporphyrin in toluene using chirp-controlled ultrashort pulses. The oscillatory features superimposed on the temporal profiles of the pump-probe transient absorption signal are affected by the chirping and energy of excitation pulses. Using chirp- and excitation energy-controlled femtosecond pulses, we are able to obtain information on the structural changes between the electronic ground and excited states based on a comparative analysis of the Fourier-transformed frequency-domain spectra retrieved from the oscillatory components with the ground state resonance Raman spectra and normal mode calculations.

Key Words : Chirped pulse, Wave packet, Zn(II)porphyrin

Introduction

Femtosecond coherent vibrational spectroscopy is based on ultrashort broadband excitation which leads to a generation of a wave packet through a superposition of vibrational levels.[1-4] A recent progress in the femtosecond coherent spectroscopy has enabled us to monitor low-frequency vibrational motions in real time, which appear as oscillatory features in temporal domain.[5,6] The initial wave packet is damped due to phase and energy relaxations and eventually the wave packet disappears. The oscillatory behavior is attributed to the wave packet motion with vibrational coherence induced by ultrashort pulse excitation, where the dynamics is usually observed by pump/probe transient absorption (TA) spectroscopy that probes the vibrational coherence in both electronic ground and excited states.[7,8] However, in usual pump/probe TA experiment, it difficult to distinguish the origin of the oscillations whether they arise from either the electronic ground and/or excited states.[9,10]

A recent development in the generation of ultrashort pulses make it possible to control the phase structure in the duration of pulses.[11,12] When all the frequency components have zero relative phase, it is called a transform-limited (TL) pulse in which all the colors arrive simultaneously. On the other hand, the negative chirp (NC) pulse has leading high-frequency parts and trailing low-frequency ones, while the positive chirp (PC) pulse has the opposite ordering in frequency distributions. Control of the phase structure of ultrashort pulses opens up new challenges beyond simple experiment with the highest possible time resolution. The idea to control the arrival time of the different frequency components of ultrashort pulses for coherent control of the temporal evolution of the wave packet has been the subject of considerable theoretical work. Thus, the femtosecond coherent spectroscopy with a control of the chirp of ultrashort pulses is ideally suited for the investigation on the potential energy surface (PES) of molecular systems. In addition, it is possible to probe a number of low-frequency vibrational modes by resonance Raman (RR) spectroscopy, where the same modes are observed in the femtosecond coherent vibrational spectroscopy.[3-6] Thus, a comparative study between the femtosecond coherent vibrational spectrum and the ground state Raman one of the molecular system is expected to give further understanding on the structural changes occurring in the excited PESs.

Recently a variety of molecular modules have been employed as construction elements in diverse molecular architectures for possible applications as molecular electronic and photonic materials.[13-15] Among these, porphyrins are one of the most attractive building block elements due to their desirable molecular characteristics such as rigid planar geometry, high stability, intense electronic absorption, and small HOMO-LUMO energy gap, as well as flexible tunability of their optical and redox properties by appropriate metalation.[16-18] Thus it is indispensable to have a deep understanding into the excited states of porphyrin molecules in various forms of molecular photonic wires, because the light signal transmission is based on the excitation energy transfer in the excited states of porphyrin molecules.[19-21]

In this work, we present time-resolved spectroscopic data on Zn(II)-5,15-diphenylporphyrin ($Zn^{II}DPP$) in toluene such as pump-probe transient absorption, coherent vibrational oscillations, and RR spectra. We also report the dependence of oscillatory features on the chirping and energy of ultrashort pump pulses to gain further insight into the structural changes occurring in the excited S_2 state of $Zn^{II}DPP$.

Experimental Section

A schematic layout for ultrafast transient absorption setup is illustrated in Figure 1a. A home-built cavity-dumped Kerr lens mode-locked Ti:sapphire oscillator is shown in a dashed box. An intra-cavity second-harmonic output (532 nm) of a diode pumped cw Nd:YVO_4 laser (4W, Verdi V, Coherent)

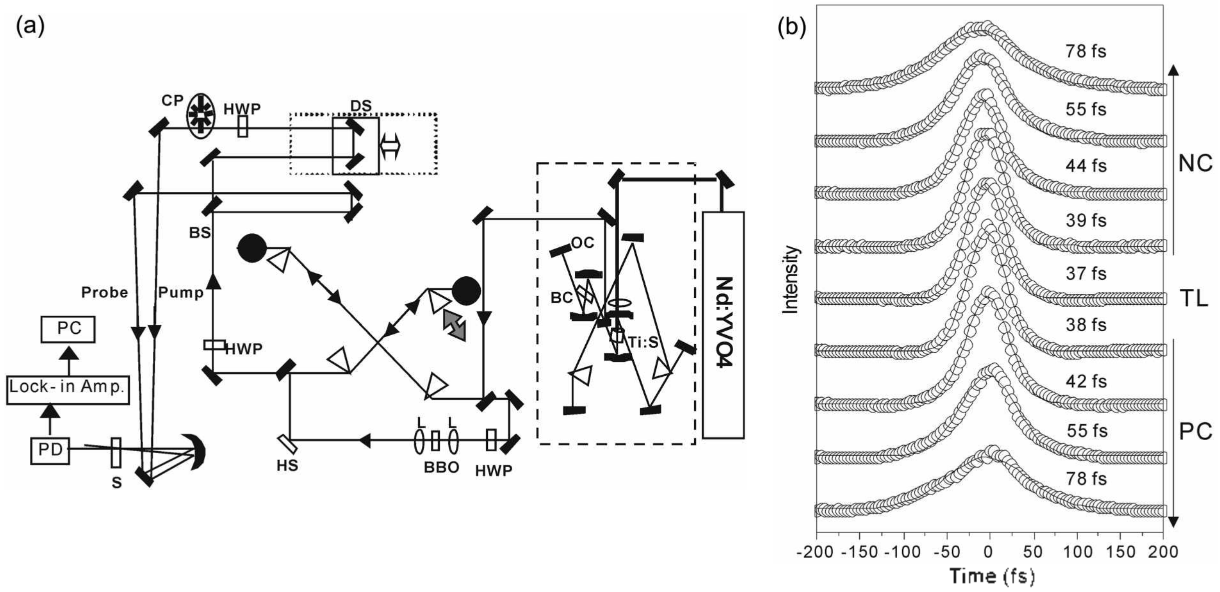

Figure 1. (a) Schematic diagram of experimental setup for pump-probe transient absorption spectroscopy. Ti:S, Titanium sapphire crystal; BC, fused silica Bragg cell; OC, output coupler; HWP, half-wave retarder; L, plano-convex lens; BBO, beta barium borate crystal; HS, harmonic separator; BS, beamsplitter; DS, delay stage; CP, chopper; S, sample cell; PD, UV-enhanced Si-PIN photodiode. (b) Temporal profiles of autocorrelation traces between pump and probe pulses and their temporal full width at half maximum of negatively chirped (upper), transform-limited (middle), and positively chirped (lower) pulses.

was focused into a Ti:sapphire crystal by a convex lens (f = 10 cm). A fused silica prism pair was used to generate cw mode-locked pulses with a compensation of intra-cavity group velocity dispersion (GVD) and to tune the wavelength. The mode-locked pulses had a typical repetition rate of 72 MHz and their averaged output power was nearly 200 mW. A 3 mm thick fused silica Bragg cell was used for an acousto-optic modulator by a RF driver (CD5000, CAMAC) for cavity-dumping, which was operated at a typical repetition rate of 200 kHz. Cavity-dumping allows the repetition rate to be reduced to avoid thermal and accumulation effects of the sample. The spectral width of dumped pulses was typically about 80 nm at the center wavelength of 820 nm. Output pulses of the cavity-dumped Ti:sapphire oscillator were compressed by an extra-cavity prism pair to compensate GVD and then focused into a 100 μm thick β-BBO (beta barium borate) crystal to generate frequency-doubled 400 nm pulses. Second-harmonic pulses were recompressed by another prism pair and then split by a broadband beamsplitter. The pump pulses were delayed by a motor-controlled translation stage (M-VP25XA, Newport) and the polarization between pump and probe pulses was adjusted to be parallel in all experiments. After overlapping of pump and probe pulses at the sample position with a very small angle, pump-induced transmittance change of probe pulses was recorded by UV-enhanced silicon photodiode (PIN-10DPI/SB, UDT) with a combination of a chopper (MC1000, Thorlabs) and a lock-in amplifier (DSP 7265, PerkinElmer). All pump-probe measurements were performed by using a quartz cell with 1 mm optical path length.

The chirp of pump pulses was controlled by changing degree of insertion of the prism for compression. The autocorrelation trace of the shortest pulses had the full-width at half-maximum (FWHM) of 37 fs (chirp free), which was broadened to 78 fs in either NC or PC pulses in our present experiment (Figure 1b) as increasing the amount of the chirp. The pulse width broadened by chirp can be well described by following equation as a function of the path-length in the prism, L.

$$T_{out} = T_0\sqrt{1+\left(\frac{4\ln 2\cdot\beta(\omega)L}{T_0^2}\right)^2}$$

where, T_{out}, T_0, $\beta(\omega)$ are FWHM of the transmitted pulse, FWHM of the transform-limited pulse, and dispersion per unit length, respectively.[7] It was found that the quadratic phase term $\Phi''(\omega) = \beta(\omega)L$ could be varied within −800 (NC) ~ +800 fs^2 (PC) by fused silica prism in our experiment. Since residual higher order chirp terms could not be removed perfectly, we refer the shortest pulse as TL pulses for the sake of convenience. Furthermore, we could neglect the higher order terms since it was well-described only by the second order dispersion in all analyses.

Steady-state absorption and fluorescence spectra were measured by a Shimatzu UV-1601 and a Hitachi F/4500 spectrometer, respectively, using a 10 mm quartz cell. Ground-state RR spectrum was obtained by using a cw He-Cd laser, a notch-filter, a 500 mm focal length monochromator (SpetraPro 500i, Roper Scientific) and a liquid nitrogen cooled CCD detector.

Zn^{II}DPP (Porphyrin Products, UT Logan) and spectroscopic grade toluene (Aldrich) were purchased and used without further purification. All measurements were performed at ambient temperature (22 ± 1 °C).

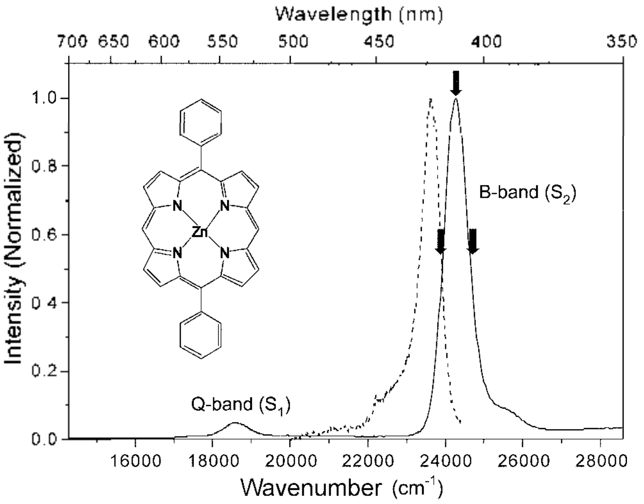

Figure 2. Steady-state absorption (solid line) and emission (dotted line) spectra of $Zn^{II}DPP$ in toluene and its structure without hydrogen atoms for clarity. Emission spectrum from the S_2 state is obtained by photoexcitation at 405 nm. Thick arrows indicate excitation wavelengths employed in pump-probe transient absorption spectroscopy.

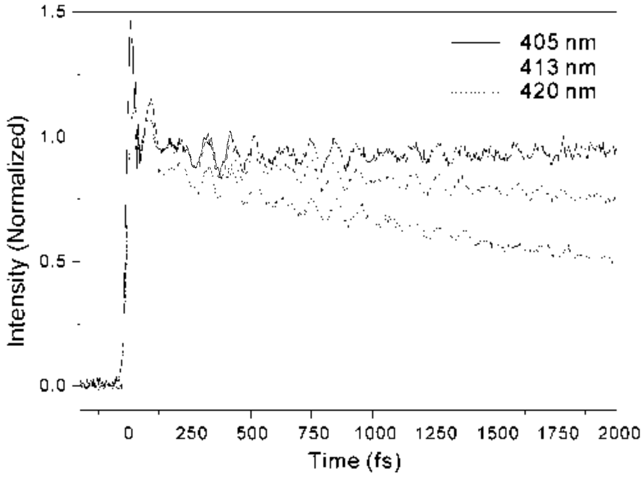

Figure 3. Transient absorption decay profiles of $Zn^{II}DPP$ by photoexcitation with transform-limited pulses at 405 (solid line), 413 (dashed line), and 420 nm (dotted line).

Results and Discussion

A. Steady-state Absorption and Fluorescence Spectra. Metalloporphyrins have well-resolved two absorption bands in the visible region. One is intense B-band (Soret band, S_2 state) located near 400 nm and the other is relatively weak Q-band (S_1 state) between 500 and 600 nm.[22] In contrast to simple B-band, there are some vibrational progressions in the Q-band. There is relatively large energy separation in metalloporphyrins between the S_2 and S_1 excited states, which are assigned to π-π^* transitions. In addition, these states are considered as a 50-50 admixture of two common excited electronic configurations $^1(a_{1u}, e_g)$ and $^1(a_{2u}, e_g)$ in accidental degeneracy and the energy surfaces of the S_1 and S_2 excited states are almost parallel.[23] Figure 2 shows the steady-state absorption and emission spectra of $Zn^{II}DPP$ in toluene. In the absorption spectrum, $Zn^{II}DPP$ has relatively strong Q(1,0) band and weak Q(0,0) and Q(2,0) bands. Emission spectrum with photoexcitation at 405 nm shows relatively strong S_2 fluorescence similar to other *meso*-substituted Zn^{II}porphyrins.[16-22,24,25] From the absorption and emission spectra, the Stokes-shift was estimated to be about 630 cm^{-1}, which is quite similar to that of Zn^{II}tetraphenylporphyrin ($Zn^{II}TPP$) indicating that the PES of $Zn^{II}DPP$ may be analogous to that of $Zn^{II}TPP$.[10]

B. Femtosecond Coherent Vibrational Spectroscopy. Femtosecond pump-probe spectroscopy gives a direct insight into the dynamics of coherent wave packet motions and subsequent vibronic relaxation processes of molecules in the condensed phase.[1-8] We have studied impulsively photoinduced vibrational coherent motions in the electronic ground and excited states of $Zn^{II}DPP$. Figure 3 shows the temporal profiles of TA changes at excitation wavelengths of 405, 413, and 420 nm, which predominantly induce the $S_2 \leftarrow S_0$ transition (Soret band). Time-resolved profiles show exponential decay components due to population transfer in addition to prominent oscillations superimposed on the TA signal due to coherent wave packet motions, which damp within 2 ps. In zero time region, coherent spikes are dominantly observed, which are usually found in one-color TA data.[10] In all TA signals, it was found that the temporal profiles are composed of two decay components with the time constants of ~1.6 ps and a few nanoseconds mainly due to contribution from stimulated emission (SE) from the excited state and ground state bleaching (GB), respectively. As like other metalloporphyrins, the S_1 state of $Zn^{II}DPP$ is formed within ~1.6 ps following the Soret band excitation and decays to the ground state on a much slower time scale.[16] The slow 1.6 ps $S_2 \rightarrow S_1$ internal conversion process for $Zn^{II}DPP$ is attributable to unfavorable Franck-Condon factors for nonradiative decay between the nearly parallel S_2 and S_1 PESs.[23] It is observed that the amplitude for each decay component depends on the pump/probe wavelengths as shown in Figure 3. As the pump/probe wavelength becomes longer, the relative amplitude for the fast decay component with the time constant of 1.6 ps increases. This is due to the fact that the SE contribution to the overall TA signal becomes larger as the probe wavelength is closer to the S_2 emission band. On the contrary, the excited-state photoinduced absorption (ESA) is also one of the important processes contributing to the TA signal, but it has opposite sign to the SE and GB processes. Although the ESA contributes to the TA signal, it is thought that its contribution is not so significant in our present data. We also observed that the amplitude of the oscillation was affected by the chirping of the pump pulses which was adjusted by a prism pair (not shown). Especially, the oscillatory components are slightly enhanced by the NC pulse excitation at 413 and 420 nm as compared with the 405 nm excitation which shows negligible dependence on the chirp of the pump pulses.

C. Fourier-transformed Frequency-domain Spectra. The dynamics of nuclear motions on PES can be directly probed

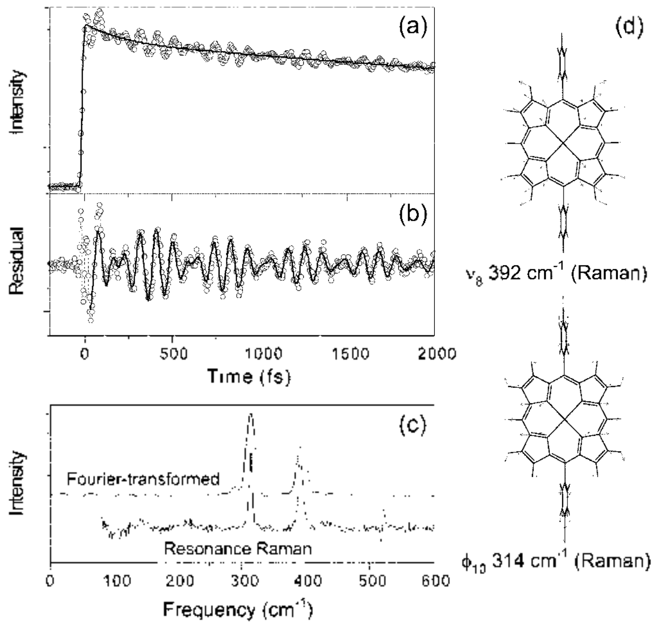

Figure 4. (a) Temporal profile of transient absorption signal of Zn^{II}DPP by photoexcitation at 413 nm with transform-limited pulses (open circles) and fitted exponential decay curve (solid line) assuming Gaussian instrumental response function. (b) Residual data (open circles and dashed line) by subtraction of fitted exponential decay curve from raw data and fitting curve (solid line) by damped sinusoidal function reconstructed by LPSVD. (c) The Fourier-transformed power spectrum from oscillatory features of the TA signal (top) and the ground state resonance Raman spectrum by photoexcitation at 441.6 nm (bottom) (d) Totally symmetric normal modes in low-frequency region calculated by semi-empirical method with PM3 level.

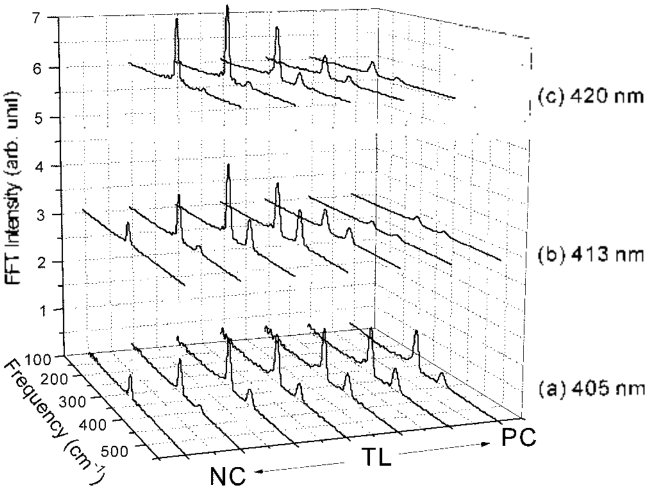

Figure 5. A series of Fourier-transformed power spectra retrieved from the oscillatory components of the time-resolved TA signals by control of the chirp and wavelength of the pump pulses.

by the femtosecond coherent vibrational spectroscopy.[5-10] The coherent wave packet motions appear as oscillatory features superimposed on the population decay. Figure 4 shows a typical procedure to retrieve the frequency domain spectra from the time-domain signals. Temporal decay signals from the TA data can be well-fitted by a convolution function composed of a Gaussian autocorrelation function and double exponential functions (Figure 4a). After an exponential contribution is subtracted by a convoluted function, residuals can be obtained, which represents the wave packet motions (Figure 4b). Then, the frequency spectra are obtained by fast Fourier-transform (FFT) of the residuals (Figure 4c). Moreover, dephasing time constants and phase relationships as well as oscillation frequencies are determined with the help of linear prediction of singular value decomposition (LPSVD) analyses.[26] Oscillation signals with the damping constants and appropriate phases can be successfully reconstructed as shown in Figure 4b. Since coherent spikes are dominant at zero time delay, they are excluded in all Fourier-transform analyses. It is noted that two significant vibrational peaks are observed in the low frequency region, which appear at 314 and 394 cm^{-1} with the dephasing time constants of 1.8 and 1.1 ps, respectively.

The RR spectroscopy provides information on the ground state vibrational modes. Figure 4c shows the RR spectrum with photoexcitation at low-energy tail of the B-band absorption of Zn^{II}DPP in toluene using 441.6 nm line from a cw He-Cd laser. In the RR spectrum two peaks are observed at 314 and 392 cm^{-1}, which are similar to the FFT spectra retrieved from the TA signals. It is worthy of noting that these two bands are quite similar in their intensities. These RR bands can be assigned to the totally symmetric A_g vibrational modes which are activated via the Albrecht *A*-term scattering.[27] Using semi-empirical calculation at PM3 level, the best candidates for these two vibrational modes are shown in Figure 4d. The RR band at 314 cm^{-1} is assigned to the ϕ_{10} mode having symmetric translational motion of two phenyl groups and a small amount of rotational motion of four pyrroles in the direction to phenyl group. The vibrational mode at 392 cm^{-1} can be assigned to the ν_8 mode which is mainly contributed by porphyrin ring breathing motion (ν(Zn-Por)) without peripheral phenyl vibrations.[28,29] This band is always strongly activated by the B-band excitation in the RR spectrum due to the π-π^* transition of porphyrin macrocycle.[10,16-20] Since these two normal modes involve relatively large vibrational motions of porphyrin ring, their intensities would be strong due to a large change in polarizability. In the previous result on Zn^{II}TPP, however, the ϕ_{10} mode is weakly enhanced presumably due to the contribution of pure phenyl translation motion without porphyrin ring vibration.[10]

Figure 5 shows a series of FFT power spectra obtained from the oscillatory features residing in the decay profiles of the TA signals by photoexcitation with chirp-controlled pump/probe pulses at 405, 413 and 420 nm. The relative intensities for the ϕ_{10} and ν_8 modes change significantly depending on the chirping of the excitation pulses at 413 and 420 nm while they remain nearly the same in the case of 405 nm excitation.

The formation of the vibrational wave packet is affected by various molecular aspects such as a displacement between the two electronic states involved in the pump/probe process and a lifetime of the excited states. The formation of the ground state wave packet is believed to be generated by the resonant impulsive stimulated Raman scattering (RISRS) process, which consists of two field-matter interactions.[2-4] From an initial interaction between the electric field of the pump pulses and the Soret transition in porphyrin, the wave packet is created in the excited PES, where it propagates within the duration of the pump pulses. Subsequent second interaction makes the wave packet bring back to the ground state with a displaced nuclear position which puts the system to vibrational coherence in the ground state. Therefore, this process is enhanced by the NC pulses since the frequency distribution of the pump pulses is ordered in time from high to low frequency. Accordingly, the NC pulses are likely to enhance the RISRS process in this experiment, which cycles population back down to the S_0 manifold while the PC pulses discriminate against this process. In addition, as excitation wavelength is closer to emission wavelength, the SE contribution becomes larger indicating that the excited state contribution increases in the oscillatory signals. The PC or NC pulses yield very different signals in spite of their similar pulse widths as shown in Figure 1b, which indicates that such difference is not due to the temporal broadening effect. The two vibrational modes at 314 and 394 cm^{-1} exhibit different dependence on the chirping and wavelength of the pump pulses. As mentioned above, these two modes are enhanced by the NC pulse excitation at the lower energy side of the Soret band as compared with the 405 nm excitation. It can be explained that a lack of chirping effect by the 405 nm excitation originates from a complicate mixing of many vibrational states in the excited state. In addition, the dependence of chirping for the 394 cm^{-1} mode is not so clear as the 314 cm^{-1} mode due to its weak intensity arising from a limited time-resolution of the present setup.

The center frequencies of the two vibrational bands at 314 and 394 cm^{-1} are plotted as a function of a degree of chirping at three excitation wavelengths (Figure 6). In the case of photoexcitation at 420 nm, significant frequency changes can be observed as compared with other excitations

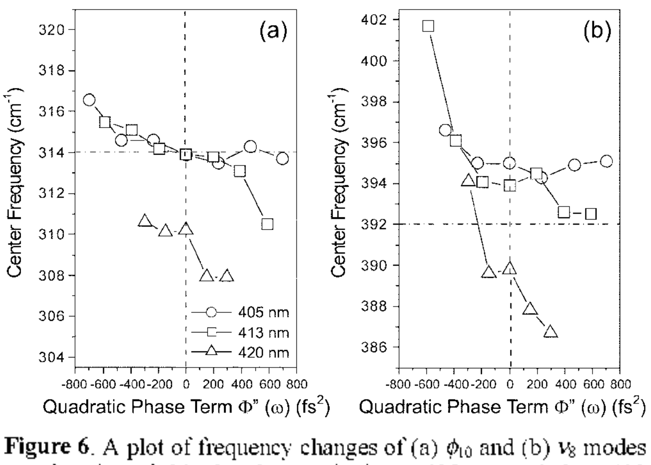

Figure 6. A plot of frequency changes of (a) ϕ_{10} and (b) ν_8 modes as a function of chirp by photoexcitation at 405 (open circles), 413 (open squares), and 420 nm (open triangles). Horizontal lines represent vibrational frequencies obtained from the ground state Raman spectrum.

and the frequencies retrieved from the TA signals are lower than those from the RR spectra. Furthermore, the vibrational frequencies are slightly shifted to even lower frequencies as the excitation pulses are more positively chirped. Since the excited state contribution is increased by the SE process with photoexcitation at the red side of the B-band and the vibrational frequencies in the S_2 state are expected to be lower than those of the ground state due to antibonding character of e_g (π^*) orbital, a slight decrease in vibrational frequencies in the FFT power spectra by photoexcitation at 420 nm mainly reflects the structural changes in the S_2 state of Zn^{II}DPP. On the other hand, the vibrational frequencies slightly shifted to higher frequency as excitation pulses are more negatively chirped in all FFT power spectra. This result implies that the ground state contribution to the wave packet dynamics becomes larger as excitation pulses are more negatively chirped. It should be noted that the vibrational frequency of the ν_8 mode in the FFT power spectrum by photoexcitation at 405 and 413 nm is always somewhat higher than that of the RR spectrum (Figure 6b). Though its origin is not clear at present time, we suggest that mode-couplings with other vibrational modes result in a slight shift to higher frequency in the FFT spectrum.[8]

Conclusion

The femtosecond coherent spectroscopy has proven to be one of the most powerful tools to investigate coherent vibrational wave packet motions in the ground and excited states. The shaped optical pulses permit us to directly differentiate the wave packet dynamics between the electronic excited and ground states. Otherwise, it is difficult to separate a pure contribution of the wave packet motions from a specific electronic state. Based on a comparative analysis between the ground state Raman spectra and the FFT spectra retrieved from the TA signals by changing the chirping and energy of excitation pulses, we are able to obtain information on the structural changes in the excited S_2 state of Zn^{II}DPP.

Acknowledgement. This work has been financially supported by the National Creative Research Initiatives Program of Ministry of Science and Technology of Korea.

References

1. Schere, N. F.; Carlson, R. J.; Matro, A.; Du, M.; Ruggerio, A. J.; Romero-Rochin, V.; Cina, J. A.; Fleming, G. R.; Rice, S. A. *J. Chem. Phys.* **1991**, *95*, 1487.
2. Bardeen, C. J.; Che, J.; Wilson, K. R.; Yakovlev, V. V.; Apkarian, V. A.; Martens, C. C.; Zadoyan, R.; Kohler, B.; Messina, M. *J. Chem. Phys.* **1997**, *106*, 8486.
3. Bardeen, C. J.; Wang, Q.; Shank, C. J. *Phys. Rev. Lett.* **1995**, *75*, 3410.
4. Bardeen, C. J.; Wang, Q.; Shank, C. J. *J. Phys. Chem. A* **1998**, *102*, 2759.
5. Rosca, F.; Kumar, A. T. N.; Ye, X.; Sjodin, T.; Demidov, A. A.; Champion, P. M. *J. Phys. Chem. A* **2000**, *104*, 4280.
6. Ye, X.; Demidov, A.; Champion, P. M. *J. Am. Chem. Soc.* **2002**,

124, 5914.
7. Misawa. K.; Kobayashi, T. *J. Chem. Phys.* **2000**, *113*, 7546.
8. Saito. T.; Kobayashi. T. *J. Phys. Chem. A* **2002**, *106*, 9436.
9. Pollard, W. T.; Dexheimer, S. L.; Wang, Q.; Peteanu, L. A.; Shank, C. V.; Mathies, R. A. *J. Phys. Chem.* **1992**, *96*, 6147.
10. Yoon, M.-C.; Jeong, D. H.; Cho, S.; Kim, D.; Rhee, H.; Joo, T. *J. Chem. Phys.* **2003**, *118*, 164.
11. Averbukh, I.; Shapiro, M. *Phys. Rev. A* **1993**, *47*, 5086.
12. Krause, J. L.; Whitnell, R. M.; Wilson, K. R.; Yan, Y. J.; Mukamel, S. *J. Chem. Phys.* **1993**, *99*, 6562.
13. Lin, V. S.-Y.; DiMagno, S. G.; Therien, M. J. *Science* **1994**, *264*, 1105.
14. Martin, R. E.; Diederich, F. *Angew. Chem. Int. Ed. Engl.* **1999**, *38*, 1350.
15. Wasielewski, M. R. *Chem. Rev.* **1992**, *92*, 435.
16. Kim, Y. H.; Jeong, D. H.; Kim, D.; Jeoung, S. C.; Cho, H. S.; Kim, S. K.; Aratani, N.; Osuka, A. *J. Am. Chem. Soc.* **2001**, *123*, 76.
17. Aratani, N.; Osuka, A.; Cho, H. S.; Kim, D. *J. Photochem. Photobiol. C* **2002**, *3*, 25.
18. Min, C.-K.; Joo, T.; Yoon, M.-C.; Kim, C. M.; Hwang, Y. N.; Kim, D.; Aratani, N.; Yoshida, N.; Osuka, A. *J. Chem. Phys.* **2001**, *114*, 6750.
19. Aratani, N.; Osuka, A.; Kim, Y. H.; Jeong, D. H.; Kim, D. *Angew. Chem. Int. Ed. Engl.* **2000**, *39*, 1458.
20. Cho, H. S.; Song, N. W.; Kim, Y. H.; Jeoung, S. C.; Hahn, S.; Kim, D.; Kim, S. K.; Yoshida, N.; Osuka, A. *J. Phys. Chem. A* **2000**, *104*, 3287.
21. Wagner, R. W.; Lindsey, J. S. *J. Am. Chem. Soc.* **1994**, *116*, 9759.
22. Gouterman, M. In *The Porphyrins*; Dolphin, D., Ed.; Academic Press: New York, 1978; Vol. I.
23. Kobayashi, H.; Kaizu, Y. In *Porphyrins: Excited States and Dynamics*; Gouterman, M.; Rentzepis, P.; Straub, K. D.; ACS Symposium Series 321; American Chemical Socienty: Washington DC, 1986; p 105.
24. Szintay, G.; Horvth, A. *Inorg. Chim. Acta* **2000**, *310*, 175.
25. Mataga, N.; Shibata, Y.; Chosrowjan, H.; Yshida, N.; Osuka, A. *J. Phys. Chem. B* **2000**, *104*, 4001.
26. Barkhuijsen, H.; de Beer, R.; Bovée, W. M. M. J.; van Ormondt, D. *J. Magn. Reson.* **1985**, *61*, 465.
27. Albrecht, A. C. *J. Chem. Phys.* **1961**, *34*, 1476.
28. Li, X.-Y.; Czernuszewicz, R. S.; Kincaid, J. R.; Su, Y. O.; Spiro, T. G. *J. Phys. Chem.* **1990**, *94*, 31.
29. Jeong, D. H.; Yoon, M.-C.; Jang, S. M.; Kim, D.; Cho, D. W.; Yoshida, N.; Aratani, N.; Osuka, A. *J. Phys. Chem. A* **2002**, *106*, 2359.